Radiofrequency heating and magnetic field interactions of fixed partial dentures during 3-tesla magnetic resonance imaging

Simel Ayyıldız, DDS, PhD,[a] Kıvanç Kamburoğlu, DDS, MSc, PhD,[b] Cumhur Sipahi, DDS, PhD,[c] Sema Murat, DDS, PhD,[d] Serkan Görgülü, DDS, PhD,[e] and Bülent Pişkin, DDS, PhD[a]
Gulhane Military Medical Academy, Ankara; Ankara University, Ankara; and Istanbul Aydın University, Istanbul, Turkey

Objective. This study evaluated the heating and magnetic field interactions of fixed partial dentures in a 3-Tesla (3T) magnetic resonance imaging (MRI) environment.
Study design. Three substructure materials (Co-Cr, Ni-Cr, ZrO_2) were used to fabricate twelve 4-retained bridges and 12 crowns. Specimens were evaluated at 3T for radiofrequency heating and magnetic field interactions. One-way analysis of variance (ANOVA) test was used to compare continuous variables of temperature change. Significance was set at $P < .05$. Translational attraction and torque values of specimens were also evaluated.
Results. None of the groups exhibited excessive heating (mean temperature change, $< 1.4°C$), with maximum increase at the end of the T-1. Moreover, in all groups, only relatively minor magnetic field interactions that would not cause movement in situ were observed.
Conclusion. The study findings indicated that patients with fixed partial dentures (single crown or bridge) fabricated from Co-Cr, Ni-Cr, and zirconia substructures may safely undergo MRI at up to 3T. (Oral Surg Oral Med Oral Pathol Oral Radiol 2013;116:640-647)

Magnetic resonance imaging (MRI) is a diagnostic imaging technique that uses static and time-varying magnetic fields (MFs) to provide tissue images through the magnetic resonance (MR) of nuclei.[1] MRI provides essential support for clinical diagnosis of soft tissue and blood flow in both medicine and dentistry.[2] The greatest advantage of MRI is its ability to provide multiplanar imaging of every part of the body without moving the patient.[3] Moreover, unlike computed tomography (CT) scans and traditional radiographs, MRI scanning is harmless to the patient, as it uses strong MFs and non-ionizing electromagnetic fields in the radiofrequency range.[4]

When placed in an MF, all substances are magnetized to a degree that varies according to their magnetic susceptibility.[5,6] Due to differences in the magnetic susceptibility of human tissue and dental alloys, metallic dental restorations may produce serious artifacts, especially in maxillofacial imaging. Metallic materials can be classified according to their degree of magnetic susceptibility as ferromagnetic (materials that have a large, positive susceptibility to an external magnetic field), paramagnetic (materials that have a small, positive susceptibility to magnetic fields), or diamagnetic (materials that have a weak, negative susceptibility to magnetic fields). Whereas ferromagnetic metals such as iron, cobalt, and nickel strongly amplify the MF, paramagnetic metals such as chromium, manganese, and aluminum only slightly amplify the MF, and diamagnetic metals such as copper, gold, zinc, lead, and carbon slightly weaken the MF.[7-9] Various materials that are used in the oral cavity for prosthetic treatment are considered ferromagnetic.[10,11]

The term *MR environment* encompasses the static, gradient, and radiofrequency (RF) electromagnetic fields that may affect implants and other devices used in the body.[11] The most immediate risk associated with the MR environment is the attraction created by the MR device between the magnet and ferromagnetic metal objects.[12] In addition to producing artifacts, metallic objects in the human body may also undergo heating, displacement, and rotation during MRI because of the electromagnetic field. During imaging, an RF pulse is used to excite

Statement of Clinical Relevance

MRI safety and the compatibility of dental alloys must always be considered before an MRI procedure. In this study, measurement of RF heating and MF interactions revealed that none of the alloys commonly used in fixed prosthodontic treatments posed danger for the patient during 3T MRI.

[a]Assistant Professor, Department of Prosthodontics, Dental Health Sciences Center, Gulhane Military Medical Academy, Ankara, Turkey.
[b]Associate Professor, Department of Dentomaxillofacial Radiology, Dentistry Faculty, Ankara University, Ankara, Turkey.
[c]Associate Professor, Department of Prosthodontics, Dental Health Sciences Center, Gulhane Military Medical Academy, Ankara, Turkey.
[d]Assistant Professor, Department of Prosthodontics, Dentistry Faculty, Istanbul Aydın University, Istanbul, Turkey.
[e]Assistant Professor, Department of Orthodontics, Dental Health Sciences Center, Gulhane Military Medical Academy, Ankara, Turkey.
Received for publication Jun 2, 2013; returned for revision Jun 21, 2013; accepted for publication Jun 27, 2013.

2212-4403/$ - see front matter
http://dx.doi.org/10.1016/j.oooo.2013.06.035

protons by an exchange of energy. The body absorbs some of this energy, and heating occurs in tissue.[1] Thus, accidents and injuries may occur with high MFs.[12] The American Society for Testing and Materials (ASTM) International and the US Food and Drug Administration (FDA) use 3 terms to define the safety of medical devices in MRI: *MR safe*, *MR conditional*, and *MR unsafe*.[13] *MR safe* refers to devices or implants that are completely non−magnetic, non−electrically conductive, and non−RF reactive, eliminating all of the primary potential threats during an MRI procedure. *MR conditional* refers to devices that may contain magnetic, electrically conductive, or RF-reactive components that may safely be operated near an MRI system. *MR unsafe* refers to devices that are strongly ferromagnetic and pose a clear and direct threat to persons and equipment within the magnet room.[13,14]

Dental treatment today involves a wide range of alloy products such as crowns, bridges, denture frames, implants, posts, pins, orthodontic brackets, wires, and amalgam,[8] and many studies have investigated artifacts generated by these materials.[7-9] MRI may also cause movement or heating of metal objects present in the body that can lead to potential health risks for patients undergoing examination. It is well known that removable dentures should be removed before MRI, as the powerful MF of the scanner can induce them to move suddenly and with great force toward the center of the MR system, causing harm to the patient as well as the device.[10]

MRI safety and the compatibility of dental alloys must always be considered before an MRI procedure[15]; however, as developments in technology have occurred, some materials now used in fixed partial dentures—such as cobalt-chromium (Co-Cr) metal substructures produced by direct metal laser sintering (DMLS) and zirconia (ZrO_2) crowns—have not been tested for MRI safety. DMLS is an additive metal fabrication technology that involves the use of a focused, high-powered Yb-fiber optic laser[16] to melt and fuse metal powder into solid parts that are built up from individual layers.[17] Zirconium dioxide (zirconia, ZrO_2) ceramics have superior mechanical properties, high flexural strength, and high fracture toughness, and over the past decade they have come into increasing use for copings and frameworks of fixed restorations.[18] The aim of the present study was to evaluate changes in temperature and MFs of fixed partial dentures fabricated from Co-Cr, Ni-Cr, and ZrO_2 in a 3-tesla MRI (3T MRI) environment and to estimate the safety of these alloys for patients undergoing 3T MRI examination.

MATERIALS AND METHODS

Preparation of specimens

A total of 36 non-carious freshly extracted human maxillary premolar teeth were selected and stored in physiologic saline solution (Isolyte 1000 mL, Eczacıbası-Baxter, Istanbul, Turkey). Cylindrical PVC rings (2 cm diameter × 3 cm length) were produced using a milling machine (Tezsan, Tos-Mas 165, Gebze, Turkey). Freshly poured autopolymerizing acrylic resin (DuraLay; Reliance Dental Mfg. Co., Worth, IL, USA) was injected into the PVC rings, and tooth specimens were embedded in the resin perpendicular to the horizontal plane 2 mm below the cementoenamel junction. After polymerization, the PVC rings containing the tooth specimens were horizontally clamped onto the rotary segment of a lathe (Tezsan, D-110, Gebze, Turkey), and the specimens were shaped using a diamond blade at 40,000 rpm under water-cooling to obtain semiconical specimens with diameters of 5 mm at the cervical level and 4 mm at the occlusal level, a crown height of 4 mm, 5° angled axial walls, and a chamfer-type finish line. Then 24 of the 36 PVC rings were fixed together in pairs using cyanomethylmethacrylate glue to obtain 12 sets of double-rings with a distance of 2 cm between tooth specimens. These double-rings were used in the fabrication of 4-unit fixed partial dentures with 2 pontics (Figure 1a), whereas the 12 single-rings were used in the fabrication of single crowns (see Figure 1b). Three types of restorative materials (Co-Cr, Ni-Cr, ZrO_2) (Table I) were used in fabrication, for a total of 6 experimental groups (n = 12), as follows: Co-Cr Crown (C-CoCr), Ni-Cr Crown (C-NiCr), Zirconia Crown (C-Zr), Co-Cr Bridge (B-CoCr), Ni-Cr Bridge (B-NiCr), and Zirconia Bridge (B-Zr).

Fabrication of restorations

Co-Cr restorations (Groups C-CoCr and B-CoCr) were fabricated using a DMLS system (M2 Cusing, Concept Laser GmbH, Lichtenfels, Germany). Tooth specimen surfaces were scanned directly using an optical scanner (Activity 102, Smart Optics Sensortechnik GmbH, Bochum, Germany), and restorations were digitally designed using three-dimensional (3D) computer-aided design (CAD). Metal substructure retainers were designed with a thickness of 0.5 mm, and pontics were designed with an occlusogingival height of 0.5 cm and a buccolingual width of 0.8 cm. After DMLS, Co-Cr bridges and crowns were annealed in an argon atmosphere at a controlled temperature in line with the manufacturer's recommendations.

Ni-Cr restorations (Groups C-NiCr and B-NiCr) were fabricated using conventional casting techniques. Casting wax was modeled onto prepared tooth specimens, and the modeled patterns were sprued, invested, and cast in an induction machine (Fornax, Bego, Bremen, Germany).

Zirconia restorations (Groups C-Zr and B-Zr) were fabricated using the 3D CAD data obtained for the

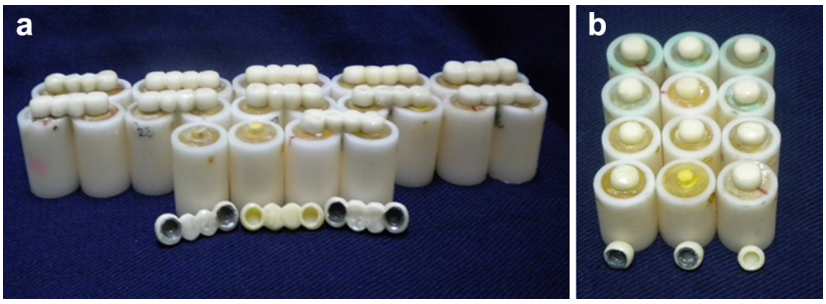

Fig. 1. (a) Co-Cr, Ni-Cr, and zirconium 4-unit fixed partial denture specimens. (b) Co-Cr, Ni-Cr, and zirconium crown specimens.

Table I. Materials and manufacturers

Group	*Material*	*Manufacturer*
C-CoCr	Co-Cr	Remanium star CL, Dentaurum, Pforzheim, Germany
C-NiCr	Ni-Cr	Remanium CS+, Dentaurum, Pforzheim, Germany
C-Zr	ZrO_2	Zirtooth O, Hass Corp, Gangneug Science Park, Gangwon, Korea
B-CoCr	Co-Cr	Remanium star CL, Dentaurum, Pforzheim, Germany
B-NiCr	Ni-Cr	Remanium CS+, Dentaurum, Pforzheim, Germany
B-Zr	ZrO_2	Zirtooth O, Hass Corp, Gangneug Science Park, Gangwon, Korea

Co-Cr restorations, with bridges and crowns milled from partially sintered blocks and sintered according to the manufacturer's recommendations.

After substructure fabrication, 2-mm thick ceramic veneers were applied using one formulation of feldspathic porcelain (Vita VM13, Vita Zahnfabrik, Bad Säckingen, Germany) for the Co-Cr and Ni-Cr groups and another formulation (Vita VM9, also by Vita Zahnfabrik) for the zirconia groups. After finishing and glazing, specimens were cemented with a temporary luting material (Life Regular Set, Kerr, Salerno, Italy) before MRI.

MRI and measurements

Heating of fabricated restorations was assessed using an infrared thermometer (Testo 845, Testo, Inc., Sparta, NJ, USA) after scanning in a 3T MRI scanner (Philips Achieva 3T X-Series, Royal Philips Electronics, Amsterdam, Netherlands). In total, 72 MRI scans were performed. Tooth specimens were placed parallel to the long axis of the coil of the MRI device[19] in a 2.5 × 2-cm concave cavity in the surface of an 8 × 4-cm cylindrical plastic container that was fixed to the bottom of a 19 × 8-cm cylindrical container at a distance of 1 cm from its inner walls (Figure 2). Both containers were filled with 2 L of 0.9% isotonic NaCl solution (Mediflex, Eczacibasi-Baxter, Istanbul, Turkey) at 22°C.

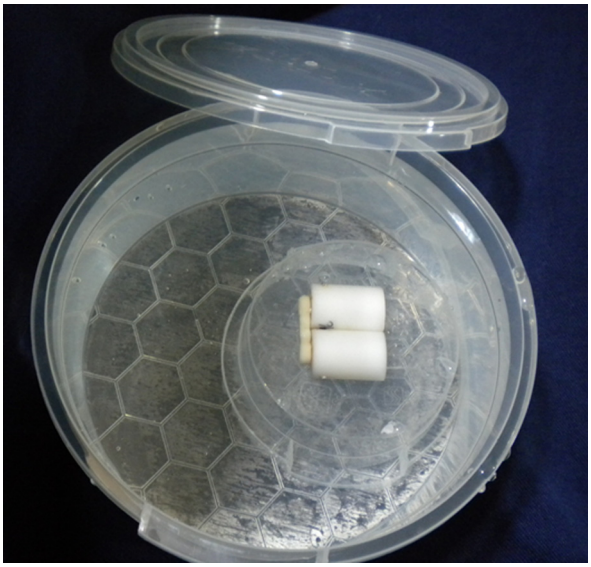

Fig. 2. A bridge specimen that was placed in the cavity of the plastic container filled with isotonic saline solution.

Just before imaging (Time 1), the temperature of both the solution and specimen (outside the container) was measured by an infrared thermometer. For the crown (C) groups, measurements were performed at the central fossae, and for the bridge (B) groups, measurements were performed at the mesial marginal side of one retainer, the distal marginal side of the other retainer, and the center of the buccal region of the pontics. The temperature of the scan room, specimens, and solution was maintained at 18°C ± 0.1°C.

Using a standard head and neck coil, specimens and plastic containers were placed on the bench of the 3T MRI device for the imaging process. Specimens were scanned with T2-weighted (T2W) turbo spin echo (TSE) in the axial and coronal planes, T1W inversion recovery (IR) TSE-based sequencing in the axial plane, and T1-3D sequencing in the sagittal plane. Technical parameters for T2W-TSE (axial), T1W-IR-TSE (axial),

Table II. Technical parameters for 3T MRI

	T2W-TSE (axial)	*T1W-IR-TSE (axial)*	*T2W-TSE (coronal)*	*T1-3D (sagittal)*
FOV (mm)	230 × 184	230 × 184	230 × 184	250 × 250
Voxel size (mm)	0.5 × 0.7 × 2	0.5 × 0.7 × 3	0.5 × 0.7 × 2	1 × 1 × 1
Slice thickness (mm)	4	4	4	<1
♯ ACQ (slices)	24	24	28	155
TE (ms)	80	20	80	3.7
TR (ms)	3000	2000	3000	8.1
Scan time (min:sec)	02:18	02:28	02:18	07:14
WFS (pix)/BW (Hz)	2.244/193.4	2.402/180.8	2.144/202.5	2.244/193.4
SAR/local head	<57%/1.8 W/kg	<57%/1.8 W/kg	<89%/2.9 W/kg	<14%/1.4 W/kg
SAR whole body/level (W/kg/normal)	<0.1	<0.1	<0.1	<0.1
NSA	1	1	1	1
Flip angle	90°-120°	90°-120°	90°-120°	8°
B1 ms [μT]	1.8	1.8	1.8	0.6

 # ACQ, number of acquisitions; *BW*, bandwidth; *FOV*, field of view; *IR*, inversion recovery; *NSA*, number of signals averaged; *SAR*, specific absorption rate; *T1W*, T1 weighted; *T1-3D*, T1 weighted three-dimensional; *T2W*, T2 weighted; *TE*, echo time; *TR*, repetition time; *TSE*, turbo spin echo; *WFS*, water-fat shift.

T2W-TSE (coronal), and T1-3D (sagittal) are shown in Table II.

Total scanning time of sequences was approximately 20 minutes. RF power output gain was adjusted manually. MRI was performed in the following sequence: T2W-axial, T2W-flair axial, T1-axial, diffusion, T2W-coronal, T1-3D-sagittal. The temperature of each specimen outside the container was measured again after T1-axial imaging (Time 2). The position of the container was maintained during measurement, and plastic tongs were used to hold the specimens to ensure that the measurements were not affected by human body temperature. Imaging continued after measurement; and after the completion of all MRI (Time 3), the container was removed from the MR device coil, specimens were removed from the container, and temperatures (outside the solution) were immediately recorded.

The statistical software program SPSS for Windows (version 15.0, SPSS, Inc., Chicago, IL, USA) was used for statistical analysis. Descriptive statistics were presented as mean, standard deviation, min-max, and 95% confidence intervals. One-way ANOVA test was used to compare continuous variables of temperature change, with a confidence level set at 95%. A post hoc Tukey test was used to compare 3 different alloys when ANOVA results were found statistically significant. A P value of $< .05$ was accepted as statistically significant.

MF interactions

After temperature measurements, specimens were evaluated for translational attraction and torque.

Translational attraction

The attraction of each specimen to the static MF was measured using the ASTM F2052-02 deflection angle method.[19] Each specimen was suspended by a 4-0 silk surgical thread (weight, 0.02 g, <1% of the specimen weight) from the 0° indicator of a plastic protractor (Figure 3). Surgical threads were attached to the center of the crown specimens and to the center of the pontics of the bridge specimens. The inner surfaces of the specimens were positioned horizontally to the bench. Deflection angles were assessed at the point of highest spatial magnetic gradient for the 3T MR scanner (690 G/cm, 71 cm distant from the isocenter). Deflection from vertical was measured to the nearest 1°. Measurements were repeated 3 times, and the average value was calculated and recorded.

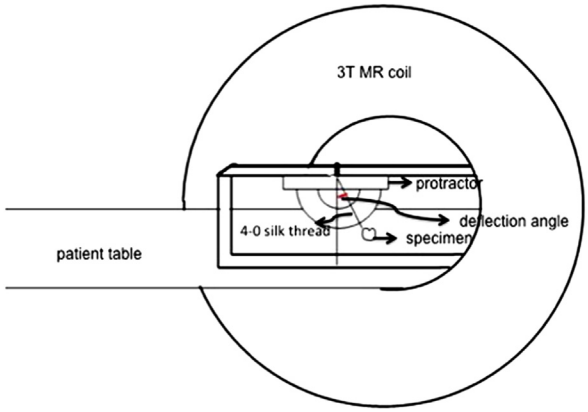

Fig. 3. Schematic illustration of translation attraction of each specimen, using the ASTM F2052-02 deflection angle method.

Torque

Torque induced by the MF was qualitatively assessed according to the method described by Shellock et al.[20,21] A millimetric grid scale was attached to the

bottom of a clear plastic container. Specimens were placed face-down in the container and perpendicular to the static MF, and the container was positioned so that the specimen was aligned at the center of the scanner, where it would be subjected to the maximum torque.

To evaluate any alignment or rotation of the specimens relative to the static MF, the test apparatus was inserted in the coil, the specimen was observed, the apparatus was removed from the coil, the specimen was rotated 45°, the apparatus was reinserted, and the specimen was observed again. This process was repeated 8 times to complete a 360° rotation of each specimen. Torque was qualitatively assessed for each specimen using the following scale[22]: 0, no torque; 1, mild torque (slight change of orientation, no alignment to the MF); 2, moderate torque (gradual alignment to the MF); 3, strong torque (rapid and forceful alignment to the MF); and 4, very strong torque (very rapid and forceful alignment to the MF).

RESULTS

RF heating

Temperature rise was observed in all groups from the beginning of 3T MRI (Time 1) until the completion of all sequences (Time 3). However, this change in temperature was not more than 1.35°C, according to mean values as shown in Tables III and IV. Also, for all groups the maximum rise in temperature occurred between Time 1 and completion of T1W-axial sequencing (Time 2), which was also statistically significant for crown (C) groups ($P < .05$) but statistically insignificant for bridge (B) groups ($P > .05$) (see Tables III and IV). A slight rise in temperature was also observed between Time 2 and Time 3 in all groups ($P > .05$).

Of the 3 crown (C) groups, maximum rise in temperature was found for the C-NiCr Group, both Time 1−Time 2 and Time 2−Time 3, according to the mean values in Table III. The greatest difference between Time 1 and Time 3 was 1.35°C for crown groups. As a result, overall RF heating for the crown groups (from Time 1 to Time 3) was statistically significant ($P < .05$). RF heating was statistically significantly higher for the NiCr groups with respect to the CoCr groups ($P < .01$). RF heating was not statistically significant for the Zr groups with respect to other groups ($P > .05$).

In all bridge (B) groups, the RF heating was statistically insignificant ($P > .05$) at each test sequence (Time 2 or Time 3) (see Table IV). As with the crown groups, maximum rise in temperature occurred between Time 1 and Time 2 for all bridge groups. The greatest difference between Time 1 and Time 2 was 0.91°C for bridge groups. RF heating values were similar in all bridge groups (see Table IV).

MF interactions

Average deflection angles ranged from 8° to 11° for the crown groups and from 9° to 13° for the bridge groups. Qualitative torque scores for all groups (1, mild torque) indicated a slight change of orientation, with no alignment to the MF in any group (Tables V and VI).

DISCUSSION

Cranial MRI at 3.0 T is generally preferred for the diagnosis of neurologic disorders,[23] ophthalmologic diseases,[24] anatomic variations,[25] disorders in pediatric patients,[26] brain tumors,[27] TMJ disorders,[28] subarachnoid hemorrhage,[29] and infections.[30] However, metal restorations, orthodontic appliances, and dentures may limit the use of cranial MRI, either by degrading the quality of the image or by causing disturbances in the image, both of which complicate accurate diagnosis and subsequent treatment decisions.[31] Besides artifacts, metallic objects in the human body may also be subject to heating, displacement, and rotation during MRI due to the electromagnetic field.[1] For this reason, MRI safety and the compatibility of dental alloys must always be considered before an MRI procedure. Metal-based materials create their own MFs. Tissues adjacent to ferromagnetic components are influenced by the induced MF of the metal and as a result do not generate a useful signal.[5,10] Not only can ferromagnetic dental alloys used in fixed partial dentures cause distortions on cranial MRI, RF heating and displacement of materials in the oral cavity are also important in terms of MRI safety.[5,6,8,10,15] In the present study, measurement of RF heating and MF interactions revealed that none of the alloys commonly used in fixed prosthodontic treatments posed danger for the patient during 3T MRI.

Co-Cr and Ni-Cr alloy fixed partial dentures are most frequently manufactured using conventional casting techniques. In recent years, modern computer-aided technologies for manufacturing individual dental prostheses have gained in popularity,[32] and both CAD and computer-aided manufacturing (CAM) technologies are frequently used in the fabrication of fixed prosthodontic substructures.[33] DMLS machines, which eliminate certain disadvantages of traditional casting such as high costs and manufacturing defects related to human error, are gaining popularity for the fabrication of Co-Cr substructures.[34] Prosthodontic clinics may also use zirconium substructures, mainly out of esthetic considerations.

The present study examined RF heating and MF interactions of Co-Cr, Ni-Cr, and zirconium-based metal-ceramic fixed partial dentures during 3T MRI. Temperature changes were similar for all the groups. Temperature rises in bridge groups were lower than

Table III. Statistical results for crown groups

Time	Crown (C) group	Mean (°C)	Standard deviation (°C)	95% confidence interval for mean (°C)		Minimum (°C)	Maximum (°C)	P*
Time 2	CoCr	18.98	.39	18.73	19.23	18.3	19.5	
	NiCr	19.17	.24	19.01	19.33	18.8	19.6	.128
	Zr	18.93	.22	18.79	19.07	18.5	19.2	
Time 3	CoCr	19.16	.41	18.90	19.42	18.3	19.7	
	NiCr	19.35	.29	19.16	19.53	18.9	19.8	.221
	Zr	19.14	.20	19.01	19.27	18.8	19.3	
Difference	CoCr	.18	.12	.10	.26	.00	.40	
Time 1−Time 2	NiCr	.45	.23	.30	.61	.10	.90	.001
	Zr	.30	.09	.24	.37	.20	.50	
Difference	CoCr	.36	.17	.25	.47	.10	.70	
Time 1−Time 3	NiCr	.63	.29	.44	.82	.20	1.10	.014
	Zr	.51	.10	.45	.58	.40	.70	

*P values belong to 1-way ANOVA test results.

Table IV. Statistical results for bridge groups

Time	Bridge (B) group	Mean (°C)	Standard deviation (°C)	95% confidence interval for mean (°C)		Minimum (°C)	Maximum (°C)	P*
Time 2	CoCr	18.81	.05	18.77	18.84	18.87	18.97	
	NiCr	18.79	.12	18.70	18.88	18.96	19.07	.331
	Zr	18.83	.11	18.80	18.91	18.98	19.10	
Time 3	CoCr	18.98	.06	18.93	19.02	19.06	19.20	
	NiCr	18.97	.12	18.87	19.05	19.13	19.23	.645
	Zr	18.98	.12	18.93	19.06	19.14	19.27	
Difference	CoCr	.30	.09	.23	.36	.20	.50	
Time 1−Time 2	NiCr	.30	.10	.24	.37	.10	.47	.693
	Zr	.33	.08	.27	.38	.20	.47	
Difference	CoCr	.47	.10	.40	.54	.33	.67	
Time 1−Time 3	NiCr	.48	.09	.41	.54	.27	.63	.970
	Zr	.48	.10	.42	.55	.30	.60	

*P values belong to 1-way ANOVA test results.

those of the crown groups. Of the 3 crown materials tested, RF heating was highest (1.35°C) for the Ni-Cr crowns according to the mean values both for Time 1−Time 2 and for Time 1−Time 3. RF heating was similar for all bridge groups, and the mean rise in temperature was not more than 1.06°C. The closer values in temperature rise among the bridge specimens as compared to the crown specimens may be due to differences in measurement techniques. Heating in crown specimens was measured through the occlusal table only, whereas heating in bridge specimens was measured at three different locations, and it is possible that a partial reduction in temperature occurred between measurements at distal and pontic sites. This would explain why RF heating was not affected by an increase in unit number in the fixed partial dentures. Ni-Cr alloys fabricated using a conventional casting technique were found to exhibit temperature increases significantly greater than those of zirconium and Co-Cr alloys. Although the temperature rise was statistically significant for crown groups in both the Time 1−Time 2 and Time 2−Time 3 sequences, this rise was not clinically significant, because it was not higher than 1.35°C.

A study by Klinke et al.[31] evaluating artifacts caused by both Co-Cr and zirconium revealed that both materials presented similar disturbances to image quality. Starcuková et al.[35] evaluated dental materials according to their magnetic susceptibility, electrical conductivity, and effect on MRI. In most previous studies, the configuration of specimens differed from that used in actual clinical practice, whereas only a few studies have investigated dental materials in their clinical form (crown configuration).[8,36] In the present study, to achieve data applicable to clinical conditions, 36 single crowns and 36 bridges were subjected to 3T MRI together with human teeth; bridges with 4-retainers (2 retainers and 2 pontics) were tested to determine if heating and torque increased with an increasing number of retainers; different alloys and manufacturing techniques were used (Co-Cr alloys manufactured using DMLS, Ni-Cr alloys manufactured using conventional casting, and zirconium

Table V. Magnetic field interactions of crown groups at 3T MRI

Group	*Deflection angle*	*Torque**
C-CoCr	9°	1
C-NiCr	11°	1
C-Zr	8°	1

*The torque values here are from a qualitative scale in which 1 = mild torque. See text for details of the scale.

Table VI. Magnetic field interactions of 4-unit bridges groups at 3T MRI

Group	*Deflection angle*	*Torque**
B-CoCr	11°	1
B-NiCr	13°	1
B-Zr	9°	1

*The torque values here are from a qualitative scale in which 1 = mild torque. See text for details of the rating scale.

substructures); and all substructures were veneered with feldspathic porcelain to accurately simulate clinical conditions. Furthermore, before imaging, each specimen was cemented using temporary cement to facilitate easy removal after imaging.

ASTM F2182-02a is a standard testing method developed for measuring RF-induced heating near a passive implant during MRI.[1] This method assumes that the devices to be tested will be located entirely inside the body and notes that, in certain cases, it may be appropriate to incorporate materials of different conductivity within the phantom.[1] However, whereas medical devices such as dental implants, orthopedic implants, stents, and neurostimulators are covered by a high volume of muscular tissue and numerous blood vessels, fixed partial dentures are not located entirely within the body but rather are located over orofacial tissue that is very close to the MR coil, and if the patient's mouth opens during imaging, the restorative device may come into direct contact with the MF.

In the present study, in line with ASTM F2182-02a data, instead of a gelled phantom material, a 0.9% saline solution was used due to the difficulties and expense involved in preparing different phantom models with heat sensors for each group. Previous similar studies performed using pure saline solution found lower temperature changes when compared to gelled phantom models.[37] However, Regier et. al.[38] tested 10 different fixed orthodontic appliances for RF heating using gelled, head-shaped phantom models and indicated that temperature changes ranged only from −0.3° to −0.2°. Another study found RF heating of a medical device fabricated from Co-Cr and Ni-Cr alloys to be less than 1°C. Thus, the results of the present study are compatible with the existing data in the literature.

In the present study, average deflection angles ranged from 8° to 11° for crown groups and from 9° to 13° for bridge groups. According to ASTM F2052-02,[19] deflection of less than 45° indicates that the magnetically induced deflection force is less than the force of gravity, and it can be assumed that the device does not pose any risk during MRI. Thus, it can be concluded that none of the devices tested represent a risk during 3T MRI. Qualitative torque measurements (Score 1) indicated only slight changes of orientation and no alignment to the MF in any of the groups tested. Therefore, it was concluded that fixed partial dentures fabricated from Co-Cr, Ni-Cr, and zirconium substructures do not present a risk for patients in a 3T MRI environment with respect to MF interaction.

This study did not evaluate changes in the microstructure of restorative cement or the effect of cement type on the study findings. However, visual inspection indicated that the provisional cement used showed no signs of dislodgement in any of the specimens. In the future, a more detailed study may be conducted to examine the effects of MR scanning at different settings and conditions on restorative cements.

CONCLUSION

The minor temperature changes and MF interactions of the specimens in the present study are considered to be within acceptable ranges. Thus, it was concluded that fixed partial dentures (single crown or bridge) fabricated from Co-Cr, Ni-Cr, and zirconia may be considered MR safe.

REFERENCES

1. American Society for Testing and Materials (ASTM) International. *Standard F2182-02a: Standard Test Method for Measurement of Radio Frequency Induced Heating Near Passive Implants During Magnetic Resonance Imaging*. West Conshohocken, PA: ASTM International; 2002.
2. Taniyama T, Sohmura T, Etoh T, Aoki M, Sugiyama E, Takahashi J. Metal artifacts in MRI from non-magnetic dental alloy and its FEM analysis. *Dent Mater J*. 2010;29:297-302.
3. Hagiwara M, Nusbaum A, Schmidt BL. MR assessment of oral cavity carcinomas. *Magn Reson Imaging Clin N Am*. 2012;20:473-474.
4. Young IR, Bydder GM. Magnetic resonance: new approaches to imaging of the musculoskeletal system. *Physiol Meas*. 2003;24:R1-R23.
5. Elison JM, Leggitt VL, Thomson M, Oyoyo U, Wycliffee ND. Influence of common orthodontic appliances on the diagnostic quality of cranial magnetic resonance images. *Am J Orthod Dentofacial Orthop*. 2008;134:563-572.
6. Harris TMJ, Faridrad MR, Dickson JAS. The benefits of aesthetic orthodontic brackets in patients requiring multiple MRI scanning. *J Orthod*. 2006;33:90-94.
7. Shellock FG, Kanal E. Aneurysm clips: evaluation of MR imaging artifacts at 1.5 T. *Radiology*. 1998;209:563-566.

8. Destine D, Mizutani H, Igarashi Y. Metallic artifacts in MRI caused by dental alloys and magnetic keeper. *Nihon Hotetsu Shika Gakkai Zasshi*. 2008;52:205-210.
9. Shafiei F, Honda E, Takahashi H, Sasaki T. Artifacts from dental casting alloys in magnetic resonance imaging. *J Dent Res*. 2003;82:602-606.
10. Hubalkova H, Hora K, Seidl Z, Krasensky J. Dental materials and magnetic resonance imaging. *Eur J Prosthodont Restor Dent*. 2002;10:125-130.
11. Shellock FG, Woods TO, Crues JV III. MR labeling information for implants and devices: explanation of terminology. *Radiology*. 2009;253:26-30.
12. Shellock FG. MR safety update 2002: implants and devices. *J Magn Reson Imaging*. 2002;16:485-496.
13. American Society for Testing and Materials (ASTM) International. *Standard F2503-08: Standard Practice for Marking Medical Devices and Other Items for Safety in the Magnetic Resonance Environment*. West Conshohocken, PA: ASTM International; 2008.
14. Shellock FG, Woods TO, Crues JV. MRI labeling information for implants and devices: explanation of terminology. *Radiology*. 2009;253:26-30.
15. Hubalkova H, La Serna P, Linetskiy I, Dostalova T. Dental alloys and magnetic resonance imaging. *Int Dent J*. 2006;56:135-141.
16. Traini T, Mangano C, Sammons RL, Mangano F, Macchi A, Piattelli A. Direct laser metal sintering as a new approach to fabrication of an isoelastic functionally graded material for manufacture of porous titanium dental implants. *Dent Mater*. 2008;24:1525-1533.
17. Bolzoni L, Esteban PG, Ruiz-Navas EM, Gordo E. Mechanical behaviour of pressed and sintered titanium alloys obtained from master alloy addition powders. *J Mech Behav Biomed Mater*. 2012;15:33-45.
18. Komine F, Blatz MB, Matsmura H. Current status of zirconia-based fixed restorations. *J Oral Sci*. 2010;52:531-539.
19. American Society for Testing and Materials (ASTM) International. *Standard F2052-02: Standard Test Method for Measurement of Magnetically Induced Displacement Force on Medical Devices in the Magnetic Resonance Environment*. West Conshohocken, PA: ASTM International; 2002.
20. Shellock FG. Biomedical implants and devices: assessment of magnetic field interactions with a 3.0-tesla MR system. *J Magn Reson Imaging*. 2002;16:721-732.
21. Shellock FG, Habibi R, Knebel J. Programmable CSF shunt valve: in vitro assessment of MR imaging safety at 3T. *AJNR Am J Neuroradiol*. 2006;27:661-665.
22. Sakai M, Shigeki A, Watanabe Y, et al. Introducer needles of peripheral intravenous catheters: assessment of magnetic field interactions with 1.5T and 3T MR Systems. *Magn Reson Med Sci*. 2009;8:181-185.
23. Sethi V, Yousry TA, Muhlert N, et al. Improved detection of cortical MS lesions with phase-sensitive inversion recovery MRI. *J Neurol Neurosurg Psychiatry*. 2012;83:877-882.
24. Menzel T, Kern R, Griebe M, Hennerici M, Fatar M. Acute posterior ischemic optic neuropathy mimicking posterior cerebral artery stroke visualized by 3-tesla MRI. *Case Rep Neurol*. 2012;4:173-176.
25. Krasny A, Krasny N, Prescher A. Anatomic variations of neural canal structures of the mandible observed by 3-tesla magnetic resonance imaging. *J Comput Assist Tomogr*. 2012;36:150-153.
26. Avula S, Mallucci CL, Pizer B, Garlick D, Crooks D, Abernethy LJ. Intraoperative 3-tesla MRI in the management of paediatric cranial tumours—initial experience. *Pediatr Radiol*. 2012;42:158-167.
27. Ramm-Pettersen J, Berg-Johnsen J, Hol PK, et al. Intra-operative MRI facilitates tumor resection during trans-sphenoidal surgery for pituitary adenomas. *Acta Neurochir (Wien)*. 2011;153:1367-1373.
28. Schmid-Schwap M, Drahanowsky W, Bristela M, Kundi M, Piehslinger E, Robinson S. Diagnosis of temporomandibular dysfunction syndrome—image quality at 1,5 and 3,0 tesla magnetic resonance imaging. *Eur Radiol*. 2009;19:1239-1245.
29. Mutoh T, Kobayashi S, Ishikawa T, et al. Pathologically confirmed cryptic vascular malformation as a cause of convexity subarachnoid hemorrhage: case report. *Neurosurgery*. 2012;70:E1322-E1328.
30. Rombaux P, Huart C, Deggouj N, Duprez T, Hummel T. Prognostic value of olfactory bulb measurement for recovery in postinfectious and posttraumatic olfactory loss. *Otolaryngol Head Neck Surg*. 2012;147:1136-1141.
31. Klinke T, Daboul A, Maron J, et al. Artifacts in magnetic resonance imaging and computed tomography caused by dental materials. *PLoS One*. 2012;7:e31766.
32. Karpuschewski B, Pieper HJ, Krause M, Döring J. CoCr is not the same: CoCr blanks for dental machining. In: Schuh G, Neugebauer R, Uhlmann E, eds. *Future Trends in Production Engineering. Proceedings of the First Conference of the German Academic Society for Production Engineering, Berlin, Germany, 8th-9th June 2011*. New York, NY: Springer; 2013:261-274.
33. Fasbinder D. Using digital technology to enhance restorative dentistry. *Compend Contin Educ Dent*. 2012;33:668-672.
34. Aboushelib MN, Elmahy WA, Ghazy MH. Internal adaptation, marginal accuracy and microleakage of a pressable versus a machinable ceramic laminate veneers. *J Dent*. 2012;40:670-677.
35. Starcuková J, Starcuk Z Jr, Hubálková H, Linetskiy I. Magnetic susceptibility and electrical conductivity of metallic dental materials and their impact on MR imaging artifacts. *Dent Mater*. 2008;24:715-723.
36. Wang W, Jiang B, Wu X, Sun JJ. Influences of three types of dental ceramic alloys on magnetic resonance imaging [abstract]. *Zhongguo Yi Xue Ke Xue Yuan Xue Bao*. 2010;32:276-279.
37. Park SM, Nyenhius CD, Lim EJ, et al. Gelled versus nongelled phantom material for measurement of MRI induced temperature increases with bioimplants. *IEEE Trans Mag*. 2003;39:3367-3371.
38. Regier M, Kemper J, Kaul MG, et al. Radiofrequency-induced heating near fixed orthodontic appliances in high field MRI systems at 3.0 tesla. *J Orofac Orthop*. 2009;70:485-494.

Reprint requests:

Kıvanç Kamburoglu, DDS, MSc, PhD
Department of Dentomaxillofacial Radiology
Faculty of Dentistry Ankara University
Ankara 06500
Turkey
Tel: 0090 312 2965632
Fax: 0090 312 2123954
dtkivo@yahoo.com; kamburogluk@dentistry.ankara.edu.tr